

# Constraining 3D facies modeling by seismic-derived facies probabilities: Example from the tight-gas Jonah Field

REINALDO J. MICHELENA, KEVIN S. GODBEY, and OMAR ANGOLA, iReservoir.com, Inc.

**S**eismic reservoir characterization is usually based on the interpretation of seismic attributes that relate to the geological feature or reservoir property of interest. If we are interested in fault geometries, a variety of geometric attributes can be used to map the details of fault distributions and constrain discontinuities and flow barriers in geological and flow-simulation models. If we are interested in reservoir properties, however, the usual approach is to estimate seismic attributes that are qualitatively related to such properties. The interpretation of the attribute focuses on the identification of “good” and “bad” areas depending on how the attribute relates to the property of interest.

This is the case, for instance, when interpreting acoustic impedance generated from seismic data.

If the goal of the project is to separate good from bad areas in terms of porosity development, all we need to do is verify that there is indeed a relation between porosity and acoustic impedance in a few wells and apply this idea to the interpretation of “highs” and “lows” in the acoustic impedance volume. Another example is the use of prestack-derived attributes, which are usually interpreted in terms “gas” and “no gas” or “sand” and “no sand” depending on the position of the data in crossplots of prestack-derived attributes at seismic scale.

On the other hand, if the goal of the project is to go beyond qualitative interpretations and build a geological model that can be later transformed into a flow-simulation model, something else besides using attributes to separate the reservoir into good and bad areas needs to be done. This is a more ambitious goal that requires more well control and other tools that can help to transform qualitative relations observed in rock physics diagnostics into quantitative variations across the reservoir.

A flow-simulation model often requires much more than a simple porosity field generated by applying a linear regression between impedance and porosity. While simple models may be all we need to simulate fluid flow in certain geological settings, complex geological or fluid variations may require additional information before meaningful fluid-flow simulation is attempted.

Fluvial sandstone reservoirs of low porosity and low permeability are a good example of reservoirs that require complex geological models to properly describe their internal architecture. These reservoirs are typically referred to in the literature as “tight.” Geological facies are the key parameter when performing geomodeling in these reservoirs for various reasons. First, thicker multistory (vertically stacked) channels are more prolific than single-story channels or individual, isolated sand bodies. Second, porosity versus permeability relations change according to facies type and, therefore, a clear understanding of facies variability becomes a prerequisite

before any porosity-permeability distribution is attempted. Third, nonpay facies are usually upscaled coarser than pay facies to keep the size of the fluid-flow models manageable while preserving important details in the interval of interest.

In this paper, we propose a statistical workflow to classify and map facies based on log and seismic data. Facies are then used as the basis to distribute porosity and permeability across the reservoir. Our approach combines geologic determinism to analyze log data with statistical approaches to analyze seismic data and indicator-based geostatistics to model single- and multistory-channel facies with appropriate spatial and geometric statistics. Unlike commonly used approaches to map facies or lithologies from seismic data based on coloring “independent” regions in seismic attribute crossplots, our approach accounts properly for overlap among different scenarios and quantifies the probability of their occurrence.

A central aspect of this paper is the generation of facies probabilities from seismic data. Since crossplots of seismic-derived attributes are the heart of our method to compute probabilities, we will start by revisiting the use of crossplots for facies/lithology classification. Then, we summarize the method to extract facies probabilities from crossplots of seismic attributes colored by facies information. Finally, we apply this method to help the characterization and modeling of a typical tight-gas reservoir, the Lance Formation at Jonah Field in Wyoming’s Green River Basin in the United States.

## Crossplotting revisited

Crossplotting is a simple but powerful tool to examine the relations between two different variables, data series, logs, or seismic attributes. By using a third variable to assign a color to each point in the crossplot, we can also assign different meanings to different regions in the crossplot that can help in the interpretation of the relations of the two main variables. Usually, the color is directly related to the reservoir property of interest. When applied to analyze seismic attributes at log scale, a colored crossplot can help us decide whether a particular combination of seismic attributes can be used to separate areas of the reservoir with the desired property from areas without it.

When performing rock physics feasibility studies at log scale to decide whether a combination of seismic attributes is adequate to separate areas of the reservoir with different properties, rock types or, more generally, different reservoir conditions, the usual approach is to look for separation of the attribute responses to the different scenarios in the crossplot domain too. When the separation is perfect, cutoffs or polygons drawn in the log-scale crossplot to separate the different scenarios are then used to interpret the corresponding attributes at seismic scale. However, perfect separation does not occur often in practice and therefore, cutoffs or polygon-based

approaches tend to misclassify many points by either leaving behind points with the desired reservoir conditions or by classifying as desirable points that are not. Besides, since absolute values and ranges of variability of attributes at log scale and seismic scale may be different, cutoffs or polygons derived from log-scale attributes may not be adequate to separate the desired scenarios when applied to the same attributes at seismic scale.

Figure 1 summarizes different cases commonly observed in practice when performing colored crossplots. Typical responses range from perfect separation of the desired scenario from the background (Figures 1a and 1g), complete overlap with clustered response for the desired scenario (Figure 1c), to complete overlap of the different scenarios with no clustering in the response (Figure 1e).

The cases shown in Figure 1 suggest that, besides separation, clustering of the response of the desired scenario with respect to the response of the background is a situation we need to examine more carefully. To achieve this goal, let's assume that the target (red dots) in Figure 1 corresponds to gas-saturated sandstones embedded in a wet background (blue dots). Even for the case of complete overlap in the response of the two cases (Figure 1c), the likelihood of finding gas-saturated sands is larger for the attribute values where the target cluster "lives" in the crossplot versus the likelihood of finding gas elsewhere.

The method we use in this paper to analyze colored crossplots goes beyond drawing polygons or extracting cutoffs to separate the scenarios of interest. It quantifies the statistical differences in the responses of the different scenarios. The next section shows how to do this in detail starting from basic probability definitions.

### Probabilities from crossplots

Briefly, we use conditional probabilities and the correspondence of the different log-scale scenarios with seismic-scale attributes sampled at well locations to estimate the likelihood of the desired scenario away from wells. Similar results can be obtained using Bayes's formula to estimate the probability if a prior estimate of likelihood is known.

A conditional probability estimates the likelihood of an event of interest given that a conditioning event is known to occur:

$$P(S) \approx P(S | A) = \frac{P(S \cap A)}{P(A)} \quad (1)$$

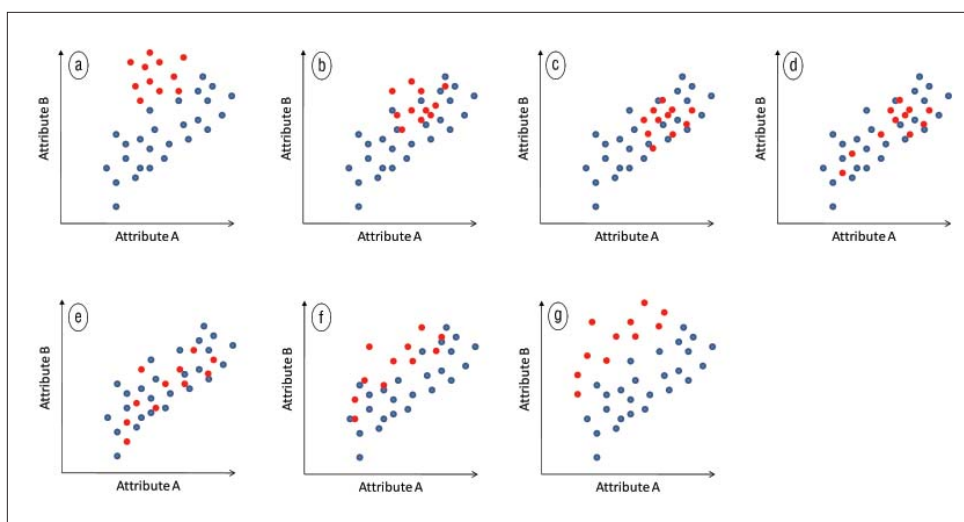


**Figure 1.** Conceptual crossplots of two seismic attributes color-coded by another variable related to the reservoir property of interest. The target (gas-saturated sandstones, for instance) is colored in red and the background is colored in blue. (a) Good separation between background and clustered target. (b) Partial separation, clustered target. (c) No separation, clustered target. (d) No separation, partially clustered target. (e) No separation, unclustered target. (f) Partial separation, unclustered target. (g) Good separation, unclustered target. Using the statistical approach described in this paper, it is possible to assign probabilities to the target even when it does not separate well from the background (cases b, c, d, and f) but the response is at least clustered or partially clustered around a certain region. This approach won't yield reliable results, however, in case (e) when the background and the target cover the same area in the crossplot. In this case the probability of the target will be the same for all attribute values.

Here,  $P(S)$  is the probability of observing the desired scenario  $S$  (e.g., a particular facies code value), and  $A$  is a conditioning event providing extra information (in our case, observed seismic attributes).

Conditional probabilities are well suited to this application because they do not require that any particular form of relationship, or even any relationship at all, exists between scenarios and attributes: If the target scenario is neither clustered nor separated from the background, as in Figure 1e, then the probability away from well locations won't change much for the entire range of attributes. Additionally, no assumptions are made about probability distributions or independence.

We define conditioning events by superimposing an  $M \times N$  grid on the attribute crossplot; each rectangle in the grid defines a conditioning event  $A_{ij}, 1 \leq i \leq M, 1 \leq j \leq N$  (see Figure 2). In notation,

$$A_{ij} = \{a_{j-1} \leq \text{Attribute } A \leq a_j \wedge b_{i-1} \leq \text{Attribute } B \leq b_i\}, \quad (2)$$

where  $a_0, \dots, a_N$  and  $b_0, \dots, b_M$  are the gridline values. We expect that samples within a scenario should have similar seismic response, so these events should tend to capture any relation between scenarios and attributes. Moreover, the conditional probabilities using these conditioning events can be estimated easily simply by counting the number of log data samples in the rectangle that are in the scenario and dividing by the total number of samples in the rectangle:

$$\frac{P(S \cap A_{ij})}{P(A_{ij})} \approx \frac{N_L(S \cap A_{ij})/N_L}{N_L(A_{ij})/N_L} = \frac{N_L(S \cap A_{ij})}{N_L(A_{ij})} \quad (3)$$

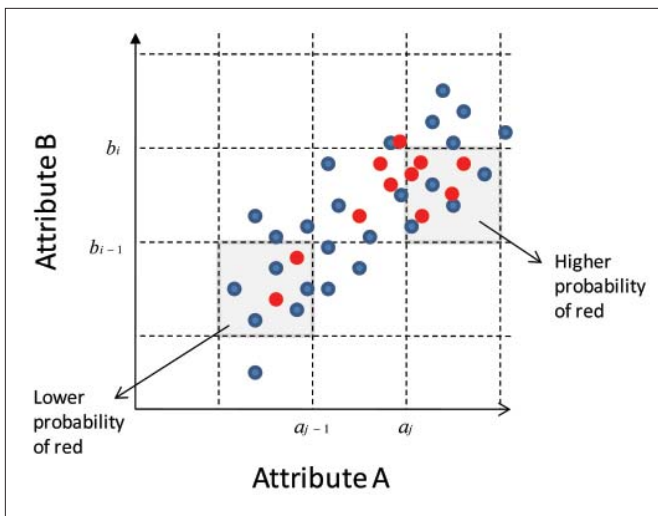


**Figure 2.** Probability estimations from crossplots. A rectangular grid is superimposed on the crossplot and individual probabilities of the different scenarios (red and blue in this example) are calculated for each rectangle. These probabilities are then assigned to the whole seismic volume.

Here  $N_L$  is the count over log data samples. This approach easily generalizes to cases where more than two attributes are believed to be related to the property of interest.

Selection of M and N for defining conditioning events involves a tradeoff and should be done on a case-by-case basis: Large M and N (small rectangles) will tend to group very closely related samples and give stronger separation, but  $N_L$  values that are too small could mean sensitivity to noise and other errors. On the other hand, small M and N (large rectangles) will group more loosely related samples and give weaker separation, but larger  $N_L$  values mean more stable estimates.

The next section explains how this method fits in a more general reservoir characterization workflow and how results derived from it can be used to map porosities and permeabilities across the reservoir.

### Jonah Field example

Jonah Field is estimated to contain 8–15 TCF of natural gas in a productive area of approximately 32 miles<sup>2</sup>. Most production comes from overpressured and ultralow-permeability sandstones of the Lance Formation, Upper Cretaceous (Maastrichtian). The Lance Formation is braided-to-meandering fluvial channels intercalated with overbank or floodplain siltstones and mudstones. The median permeability of sandstones within the Lance Formation is about 0.01 md and median porosity is about 8%. The top depths of the Lance Formation range between 8000 and 10,000 ft and the gross pay interval ranges between 2800 and 3500 ft. Significant changes of sandstone occurrence and thickness in closely spaced wells provide strong evidence for a high degree of vertical and lateral depositional compartmentalization in the Lance Formation. Strong compartmentalization translates into infill well performances that are highly variable and difficult to predict. For this reason, a reliable estimation of the facies distribution within the Lance is crucial for the development of the field. More details about Jonah Field can

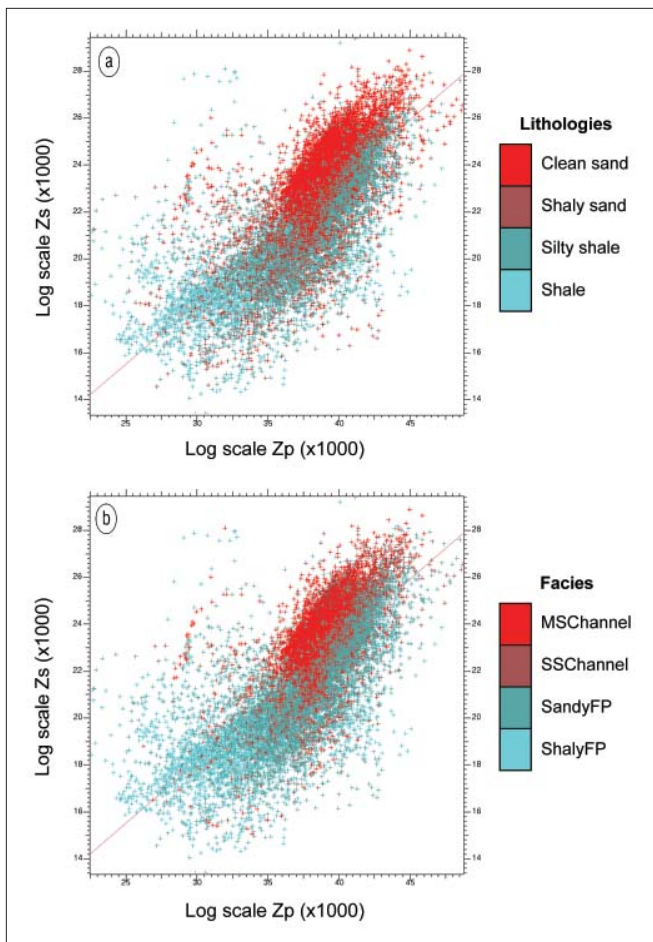


**Figure 3.** Crossplots of log scale acoustic versus shear impedance within the Lance Formation at three well locations. Four lithologies can be estimated from petrophysical analysis: clean sand, shaly sand, silty shale and shale. These lithologies can be further grouped into facies using rules based on thickness and dominant lithology: Multistory channels (clean sands of thickness greater than 15 ft), single-story channels (clean sands between 15 ft and 5 ft), sandy floodplains (clean sands less than 5 ft) and shaly floodplains (shales). Crossplot (a) is color-coded by lithologies and crossplot (b) is color-coded by facies. Notice how facies are easier to separate than lithologies since clean sands show more dispersion in the crossplots than thicker channel facies, and are probably easier to detect with seismic data.

be found in a classic compilation of papers by Robinson and Shanley (2004). Additional information about characterization and fluid flow simulation results in Jonah Field can be found in Michelena et al. (2009).

The results presented in this paper were obtained from 9.7 miles<sup>2</sup> of the field using approximately 40 wells to both calibrate the seismic response and build the geomodel. Characterization of the facies geometry focused on the identification of pay and nonpay facies using core and well-log data. Pay facies consist of single- and multistory channels. Single-story channels correspond to sandstone bodies accumulated in point bars associated with meander belts aligned NW-SE. Nonpay facies consist of floodplains, fine-grained shaly sandstones, and thin sandstones. These last two facies are interpreted to be small crevasse splays and levees.

Facies geometries were characterized using three differ-

ent methods to capture different scales of variability across the field: (1) local, log scale around each well; (2) global, log scale for the whole section; and (3) seismic scale for the whole section. The workflow to characterize facies at these different scales follows.

**Petrophysics.** Petrophysical analysis and modeling was the starting point of the reservoir characterization workflow. The result of this step is a normalized set of enhanced logs that were used for seismic-well calibration, stratigraphic interpretation, and facies classification. Well-log derived porosities were calibrated with core data.

**Log-scale lithology and facies classification.** Determination of lithology and facies associations was the next step. A set of rules designed to classify all lithologies (coal, shale, silty shale, shaly sandstone, and clean sandstone) based on density and vshale logs was applied to all wells. Results were carefully checked for misclassifications and calibrated with core data. Using these lithology logs, facies associations were then developed based upon the dominant lithology and thickness of each interval. Three facies were identified depending on the thickness of the clean sand interval: multistory channels, single-story channels, and silty-sandy floodplains (from thickest to thinnest, respectively). The term shaly floodplain was applied to nonpay intervals where shales and/or coals were the dominant lithology. See caption of Figure 3 for more details about the facies association rules.

**Crossplots of impedances at log scale.** Rock physics analysis of well-log data indicates that seismic attributes derived from 3D prestack seismic data may be good indicators of the presence of sands in the Lance Formation. Figure 3a shows how clean sands tend to cluster in one area of the P-impedance versus S-impedance crossplot for three wells in the field, but some sands are still present in other areas of the crossplot and the overlap between sands and other lithologies is substantial. Figure 3b shows the crossplot of acoustic versus shear impedance colored by facies. Notice how there is less dispersion in the channel response across the crossplot in Figure 3b when compared with the sand response shown in Figure 3a, which suggests that acoustic properties of thick sand bodies are more consistent than those of individual, isolated sands. Notice also that acoustic impedance alone is not enough to separate different lithologies or facies. The fact that most sands or channels tend to cluster in one area of the crossplot served as the basis to justify performing prestack acoustic and shear-impedance inversion in a 100 mile<sup>2</sup> area in the middle of the field.

**Stratigraphy.** Stratigraphic correlations and seismic interpretation are very difficult at Jonah Field due to rapid lateral changes in lithology within the Lance Formation. For this reason, only major markers clearly visible in both facies logs and seismic data were correlated in this section: TFU0, KL\_Upper and Mesaverde. These markers separated the producing zone in two main intervals: Unnamed Tertiary at the top and Lance Formation at the bottom. Two iterations were required to ensure consistency between seismic horizons and well markers.

**Vertical facies proportion curves.** Once the seismic-guided

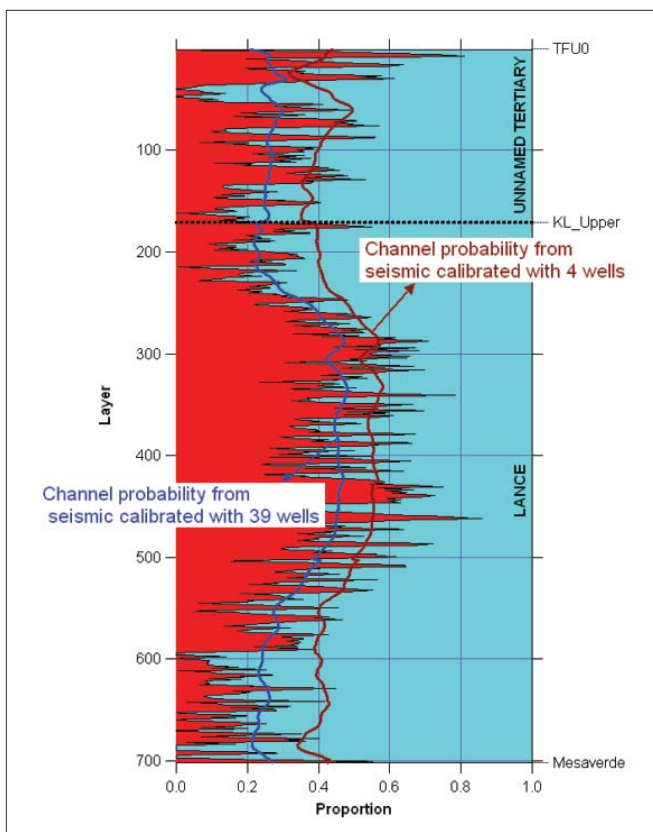


**Figure 4.** Channel facies (red area) from vertical proportion curves (VPC) computed from 39 wells versus average channel probabilities extracted from seismic data calibrated with 39 wells (blue curve) and 4 wells (red curve). Seismic-derived probabilities follow the same trend as the VPC. These results indicate that channel facies are more abundant in the Upper Lance interval. For all 39 wells, the interval between the TFU0 marker and Mesaverde marker was divided into 705 layers to compute the vertical proportion curves. The average layer thickness is 5 ft.

stratigraphic correlations were completed, the intervals of interest were divided into a fixed number of layers for all wells in the study area. Layer thickness was variable, but averaged approximately 5 ft. The total thickness of each facies for all wells was calculated for each layer and the relative proportions of the different facies by layer were computed. The result of applying this process to channel and nonchannel facies at each well is shown in Figure 4. These curves (known as “vertical facies proportion curves”) are used to estimate and constrain the relative amounts of each facies in each layer of the geomodel. After examining the relative proportions for each depth interval, it is evident that in terms of spatial variability the Upper Lance Formation shows more continuous and thick channels than the overlying Unnamed Tertiary and the underlying Lower Lance. As shown in Michelena et al. (2009), these differences in channel variability and thickness have a direct impact on gas recovery for the different intervals and sections of the field.

**Crossplot of impedances at seismic scale.** Acoustic- and shear-impedance volumes were converted to depth by using a velocity model that precisely matched all well markers at all wells used for the study. Only four out of the 40 wells used in

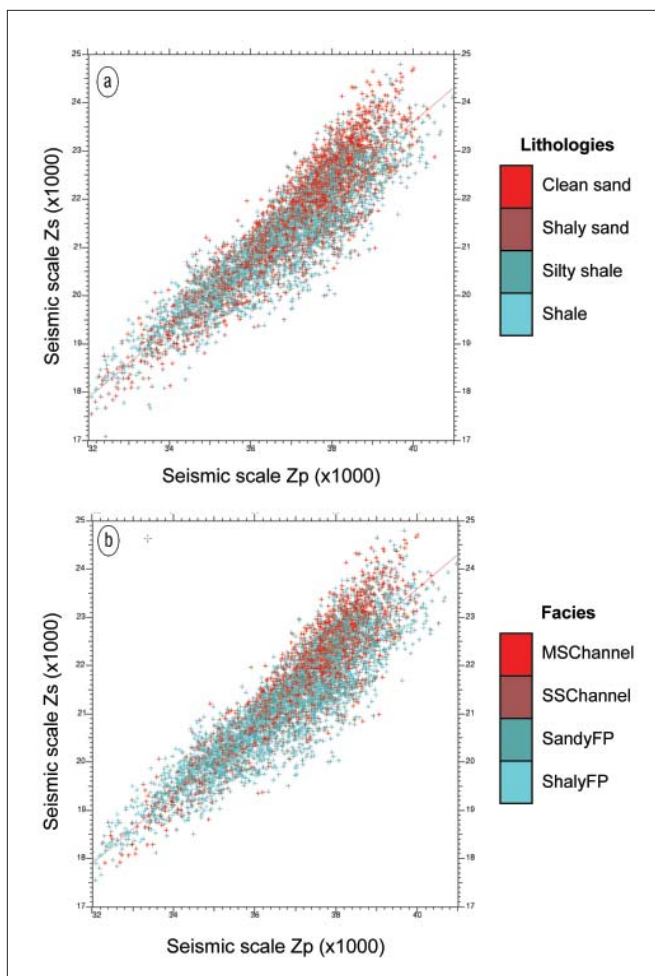


**Figure 5.** Crossplots of seismic-scale acoustic versus shear impedance within the Lance Formation at 39 well locations. The fact that clean sandstones (a) show more dispersion in the crossplots than thicker channel facies (b) indicates that facies are easier to separate than lithologies by using seismic data. Only one sample every 50 ft has been used to simplify the display of these crossplots. However, all samples were used to estimate the channel probabilities.

this study had sonic logs and, therefore, well markers played a key role in the construction of the velocity model. Impedance volumes in time were converted to  $110 \times 110 \times 5$  ft cell size impedance volumes in depth. After time-to-depth conversion, seismic-scale acoustic and shear impedances were extracted at each well location at the well-log sampling rate. Figures 5a and 5b show crossplots of seismic-scale impedances colored by log-scale lithology and facies flags respectively. As expected from the analysis of log-scale impedances (Figure 3), clean sands and channel facies (in red) tend to cluster in the area of the crossplots that corresponds to higher impedances and lower  $V_p/V_s$  ratios. The small separation between channel and nonchannel facies observed at log scale is smeared off at seismic scale, but the channel response is still more clustered than the clean-sand response, as observed also at log scale. Notice that the impedance ranges of the crossplots in Figures 3 and 5 are different. This indicates that a polygon drawn around channel facies in the crossplots at log scale will misclassify many points when also used to classify facies at seismic scale.

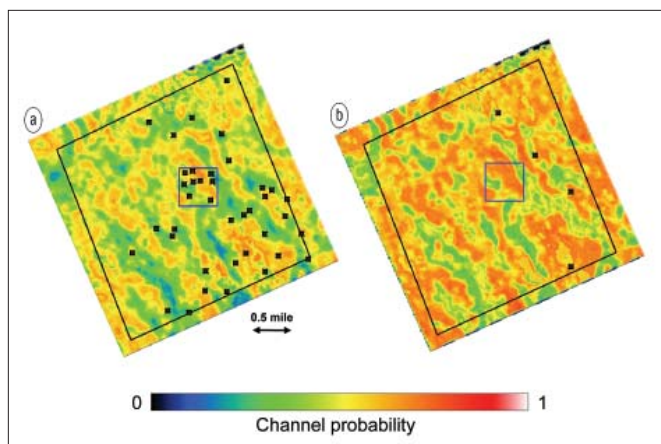


**Figure 6.** Depth slices within Lance Formation of channel probabilities extracted from 3D channel probability cubes estimated from seismic-scale acoustic and shear impedances and log scale facies: (a) using 39 wells and (b) using 4 wells. Both slices are extracted at the same depth. Locations of wells used to compute the probabilities are black. Both maps show similar trends, but the one created with 4 wells (b) tends to be more optimistic since these particular wells are in a region with higher overall sand content. A detailed reservoir simulation model was built in the area within the blue square.

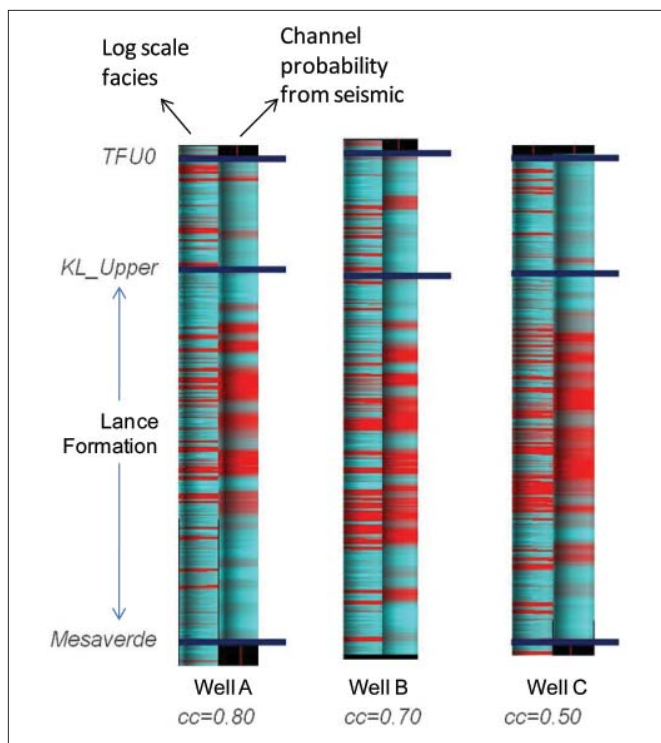


**Figure 7.** Comparison of log scale facies with channel probabilities estimated from seismic data for 3 different wells. Log scale facies (left at each well) vary from 1 (shaly floodplains, cyan) to 4 (multistory channels, red). Channel probabilities from seismic (right figure at each well location) vary from low (cyan) to high (red). The correlation coefficients (cc) at the bottom of the figure are computed using a smooth facies log and the channel probability from seismic extracted at each well. Notice how channel probabilities correlate well with thicker stacks of channels, even though these channel probabilities are not able to separate individual multistory channels observed at well locations. Misalignments between facies logs and channel probabilities from seismic are due to inaccuracies in the time-to-depth conversion which is poorly constrained within the Lance interval.

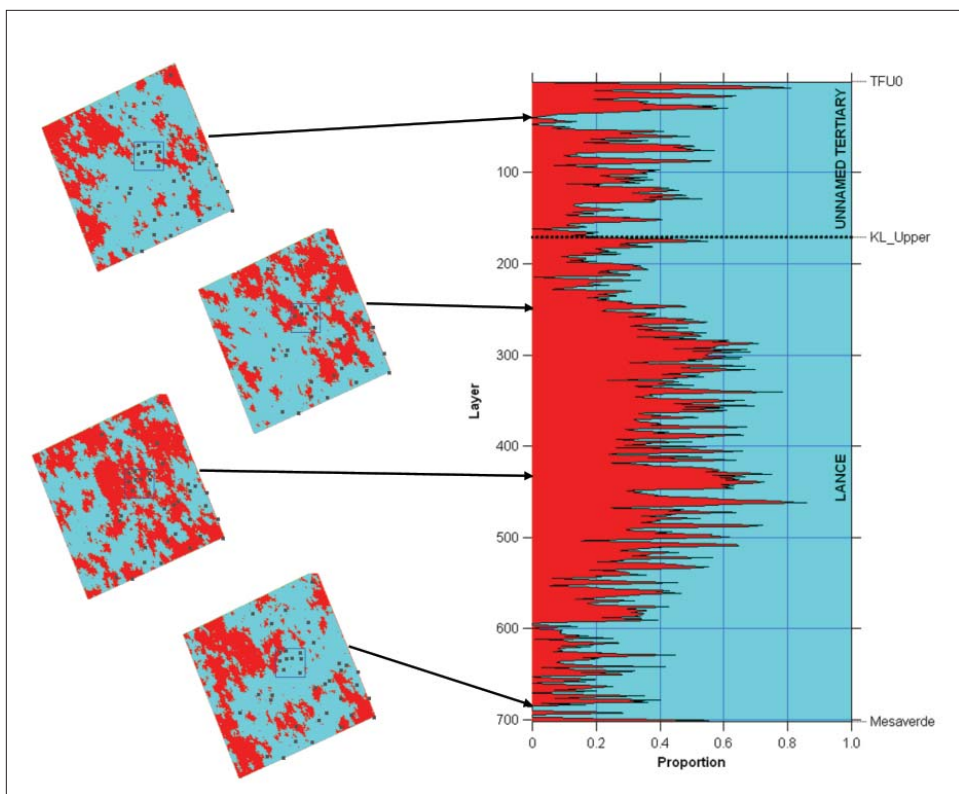


**Figure 8.** Examples of facies maps extracted from layers of the 3D facies model built using log and seismic data. By definition, proportions of channel (red) and nonchannel (cyan) facies in the maps are consistent with proportions indicated by the vertical proportion curves for the corresponding layer.

If the polygon is drawn directly in seismic-scale crossplots, the amount and connectivity of channel facies will be overestimated.

**Facies probabilities from seismic.** 3D probabilities of channels based on acoustic- versus shear-impedance crossplots were computed using the approach described in the section “Probabilities from crossplots” above. Figure 6 shows depth slices within the Lance Formation extracted from the channel probability cubes calibrated using facies logs from 39 and 4 wells, respectively. Both slices show similar trends, but the one extracted from the probability cube built with 39 wells estimates show overall lower probabilities. The fact that probabilities estimated by calibrating with 39 or 4 wells show similar variability suggests that this technique can yield useful results in areas with sparse well control, provided these few wells capture adequately the overall seismic response of the different facies.

Layer averages of facies probabilities cubes are the seismic resolution equivalent to the log-based facies proportion curves. Figure 4 compares the average probabilities (for 39 and 4 wells) computed for each stratigraphic layer with the channel proportions calculated using facies logs in the same area. Notice that seismic-derived probabilities follow the same trend as the channel, vertical proportion curve. The consistency of these two pieces of information suggests that seismic-derived probabilities can be used as secondary data to constrain the lateral distribution of facies in the geomodel. The fact that the probabilities estimated using 39 wells are closer to the ac-

tual proportions curves than the probabilities estimated with four wells suggests that adding more wells helps obtain better absolute probabilities.

Figure 7 compares log-scale facies with channel probabilities from seismic at three wells. Even though channel probabilities do not separate individual multi-story channels at wells, they do correlate with thicker stacks of channels.

**3D facies modeling.** The first step of the geomodeling process consisted of gridding seismic horizons in depth. Second, a high-resolution ( $66 \times 66 \times 5$  ft) 3D stratigraphic grid was constructed to model the fine-scale vertical heterogeneity of the reservoir. Areal experimental variograms were estimated from seismic-derived facies probability cubes and vertical variograms were estimated from well logs. The facies probabilities estimated from seismic impedances in depth were mapped onto the

stratigraphic grid and rescaled layer-by-layer to match the global vertical proportion curves. This result was then used as secondary data to constrain the lateral distribution of facies using sequential indicator simulation (Goovaerts, 1997; Deutsch, 2002). Besides incorporating the lateral channel variability observed in the seismic data, facies models built in this fashion also honor both local facies information from well data and global facies proportion curves. Figure 8 shows the result of the facies distribution in 3D for selected layers of the model. Notice how the facies distribution honors the facies proportions calculated from well data and reflects the heterogeneous nature of the fluvial environment.

**Porosity and permeability distribution.** Porosity was distributed on the seismic-constrained facies models using facies-dependent variograms and sequential Gaussian simulation while also honoring log data and porosity statistics per facies. Porosity in nonpay facies was set to zero. No attempt was made to use acoustic impedance as secondary data to map porosity because, as shown in Figure 3b, acoustic impedances alone do not discriminate between channel and nonchannel facies in Jonah Field. Permeability was distributed using a core-derived porosity-permeability cloud transform. For flow simulation, the fine-scale geomodel was then upscaled to preserve details of vertical heterogeneous channel distributions and property variations.

## Discussion and conclusions

We have presented a workflow to estimate facies probabilities

from log and seismic data and use this information to constrain the facies distribution in the reservoir. Our workflow starts by performing careful petrophysical and geological analysis which results in a set of facies logs that are used to help the characterization of facies at three different scales. Local facies curves and vertical proportion curves are treated as hard data whereas seismic derived probabilities are used as soft constraints when building the geomodel and distributing facies using sequential indicator simulation.

A key step in the workflow is the estimation of facies probabilities from seismic data. Our approach estimates the likelihood of different scenarios from crossplots of seismic attributes colored by the property of interest. Unlike polygon- or cutoff-based approaches, our approach accounts for overlap of the different scenarios. The example from Jonah Field suggests that lateral averages of facies probabilities derived in this fashion are the analogs at seismic scale of vertical proportion curves estimated from log data. Vertical proportion curves are used to rescale facies probabilities from seismic before these probabilities are used to constrain facies distribution in the geomodel.

Facies are the key parameter when modeling tight-gas reservoirs. Besides determining which areas of the reservoir are more prolific, controlling the relations between porosity and permeability, and helping in the upscaling process, our examples from Jonah Field also show that facies are easier to detect than individual lithologies when using seismic attributes. Crossplots at both log and seismic scale from Jonah Field show that thick channel facies show less dispersion in attribute crossplots than individual sand bodies. This observation suggests that acoustic properties of small sand bodies are less consistent and more variable across the reservoir than those of thicker stacked sands. Probabilities of channels estimated from seismic data at Jonah Field correlate well with stacks of multistory channels.

**Suggested reading.** *Geostatistical Reservoir Modeling* by Deutsch (Oxford, 2002). *Geostatistics for Natural Resource Evaluation* by Goovaerts (Oxford, 1997). “Infill well evaluations of Jonah Field tight gas: characterization and simulation of complex architectural elements” by Michelena et al. (*First Break*, 2009). *Jonah Field: Case Study of a Giant Tight-Gas Fluvial Reservoir*, edited by Robinson and Shanley (AAPG Studies in Geology 52, 2004).

#### TLE

*Acknowledgments:* We thank EnCana Oil & Gas USA for permission to publish this paper. We also thank our former coworker Juan Florez (now with BP) for his ideas about facies probabilities in early stages of this work. Thanks to Mike Uland for his careful petrophysical analyses and suggestions to improve the quality of this work.

*Corresponding author:* Michelena@ireservoir.com